Am J Transl Res 2020;12(6):2640-2651
www.ajtr.org /ISSN:1943-8141/AJTR0102908

Original Article

Gender differences in tibial fractures healing in normal and muscular dystrophic mice

Zhenhan Deng[1,2], Xueqin Gao[1,3], Xuying Sun[1], Yan Cui[1], Sarah Amra[1], Johnny Huard[1,3]

[1]Department of Orthopaedic Surgery, McGovern Medical School, University of Texas Health Science Center at Houston, Houston, TX 77054, USA; [2]Department of Sports Medicine, The First Affiliated Hospital of Shenzhen University, Shenzhen Second People's Hospital, Shenzhen 518035, Guangdong, China; [3]Center for Regenerative Sports Medicine, The Steadman Philippon Research Institute, Vail, CO 81657, USA

Received September 27, 2019; Accepted April 25, 2020; Epub June 15, 2020; Published June 30, 2020

Abstract: Duchenne muscular dystrophy (DMD) patients have a high fracture risk and poor fracture healing. The dystrophin$^{-/-}$ (*mdx)* mouse is a murine model of DMD and exhibits delayed bone fracture healing. Since our research team has shown that adult stem cells, such as muscle-derived stem cells, display a gender difference in their osteogenic potential with the male cells being more osteogenic, we hypothesize that a potential gender differences may exist during bone healing in normal and *mdx* mice. To test this hypothesis, wild-type (WT) and *mdx* mice underwent tibial fracture surgery and microCT live scanning biweekly. The mice were sacrificed at 6 weeks post-surgery and the calluses were collected for histological analysis. To further investigate the mechanism, another two sets of mice were sacrificed at 10 days after fracture for RNA extraction and gene expression analysis and histology. MicroCT results showed, at 6 weeks post- surgery, the calluses were larger but showed less remodeling in both normal and *mdx* male mice when compared to females, at the same time point. However, females had higher callus bone volume density and an increase in osteoclast (OCs) number. At 10 days after fracture surgery, male mice had formed larger calluses, whereas females formed well-remodeled calluses with more osteoblasts and a greater bone area for both WT and *mdx* mice. Higher IGF-1 expression was observed in male *mdx* mice when compared to their female counterparts, whereas female WT mice had higher BMP-9 expression when compared to WT males. In conclusion, male mice formed larger bone calluses than females during tibial fracture healing for both WT and *mdx* mice. This may be attributed to higher IGF-1 expression, activation of Wnt/β-catennin signaling pathway and greater OB numbers during callus formation. Female mice achieved better bone remodeling in the regenerated bone with higher bone quality due to increased OC numbers that promote faster remodeling of the fracture calluses, and higher BMP-9 expression levels. Therefore, gender is one of many factors that need to be considered for both animal and human bone research.

Keywords: Fracture healing, muscular dystrophy, gender difference

Introduction

Duchenne muscular dystrophy (DMD) is an X-linked, recessive, degenerative muscle disorder caused by the lack of dystrophin expression at the sarcolemma of muscle fibers. DMD patients develop progressive muscular weakness, and cardiac and respiratory failure, which usually leads to premature death [1]. DMD patients exhibited scoliosis, osteopenia, osteoporosis, and decreased build-up of cortices in long and flat bones, resulting in an increase in the occurrence of fractures [2, 3]. One previous study reported that, of 71 DMD boys studied, 44% overall and 67% of those over 16 had suffered at least one fracture [4].

Dystrophin-deficient (*mdx*) mice are a widely used mouse model for studying human DMD [5, 6]. This animal model exhibits myopathogenic lesions characteristic of those seen in DMD patients [7]. The *mdx* mice also exhibit inferior bone quality [8]. Furthermore, it has been reported that fracture healing is delayed in *mdx* mice, which is caused by chronic inflammation and decreased vascularization in the early stage of repair [6].

Previous studies in our lab have shown that there are gender differences in the differentiation potential of murine muscle-derived stem cell (MDSC)-mediated bone formation. Male MDSCs are more osteogenic and chondrogenic

in vitro, and regenerate more bone and cartilage *in vivo* [9-11]. In fact, we have observed that male MDSCs form more ectopic bone when stimulated with BMP4 and show improved calavarial defect healing compared to MDSCs from females, independent of the gender of the host or sex hormones. However, the contribution of gender to fracture healing differences in normal and *mdx* mice has not been extensively studied. Therefore, the purpose of this study was to investigate gender differences in tibial fracture healing in normal and *mdx* mice and to identify potential mechanisms which might be involved in the gender difference.

Materials and methods

Animals

Two-month-old wild type C57BL/10J (WT) and *mdx* (Dystrophin$^{-/-}$) mice were purchased from the Jackson Laboratory and then housed and bred in the animal facility in the University of Texas Health Science Center at Houston, Houston, Texas (UTHealth). The Institutional Animal Care and Use Committee of UTHealth approved all animal procedures (AWC 15-0073).

Tibia fracture surgery

The tibia fracture surgery was performed according to a protocol previously reported with modifications [12]. Briefly, WT and *mdx* mice were anesthetized by 2% isoflurane, the right tibia was exposed and muscles were dissociated. A pilot hole was made with 0.7 mm drill burr in the proximal tibia distal from the growth plate. Then, the tibia were cut in the mid-shaft using a 0.7-mm drill burr, with saline irrigation during the drilling process to avoid overheating. After the tibia was broken, a sterile 28-gauge needle was inserted into the tibial medullary cavity for internal fixation through the pilot hole, and the broken bone ends were aligned to normal anatomical orientation. Buprenorphine (0.05 mg/kg subcutaneously) was applied for post-surgical analgesia at postoperative day 1 and 3.

MicroCT scanning and analysis for fracture healing

The mice were anesthetized by 2% inhaled isoflurane and then the fracture sites were analyzed by live microCT scan via a Scanco Viva CT 40 system (Scanco Medical, Switzerland) at day 1 and weeks 2, 4, and 6 post-surgery. The scanning parameters were 30 μm resolution, 70 kVP and 112 μA. To analyze the fracture healing, 150 continuous slices (75 slices up and 75 slices down from the fracture site) (breaking point) covering the middle part of the newly formed bone callus were segemented from the native cortical bone by manually drawing contours to define the view of interest of the calluses. 3D images of both the entire fractured tibia and the segmented newly formed bone callus were reconstructed. The bone microarchitectural parameters for callus trabecular bone, including total volume (TV), bone volume (BV), bone volume fraction (BV/TV), bone volume density, trabecular number (Tb.N), and trabecular separation (Tb.Sp) were automatically generated by microCT software. Nomenclature followed the guidelines of the American Society of Bone and Mineral Research [13, 14]. A micro CT Gauss=0.8, Sigma=1, and threshold of 163 were used for all samples for quantification.

Histology

The mice were sacrificed at 10 days or 6 weeks post-surgery, and the entire tibia was dissected. Then, tissues were fixed in 10% neutral buffered formalin (NBF) for 72 hrs. The fixed tissues were decalcified using 10% ethylenediaminete traacetic acid (EDTA) plus 1% sodium hydroxide for 4 weeks, the internal fixation pins were carefully removed, and then tissues were processed by dehydrating in ethanol, infiltrating with xylene, and paraffin-embedding. Sections were cut at 5-μm thickness using a microtome, deparaffinized using xylene, and hydrated via ethanol gradient and water for further histology.

Hematoxylin and eosin (H&E) staining was performed to reveal the general morphology of the fracture site. Herovici's staining was used to measure the major bone matrix collagen type I. In brief, slides were deparaffinized and incubated in polychrome solution for 5 min at RT. Then, the slides were removed and immediately placed in 1% acetic acid for 2 min, rinsed with 100% ethanol, and then dehydrated to xylene [15-18]. Alcian blue staining (IHC World; http://www.ihcworld.com/_protocols/special_stains/alcian_blue.htm) was performed to investigate the endochondral bone repair of the fractured

tibia. Cartilage formation was measured by the ratio of cartilage area (blue stained) over callus area (red stained) in each section using Image J software, according to the literature [19, 20].

Immunohistochemistry

For immunohistochemistry staining, after deparaffinization, different antigen retrieval methods were used for different primary antibodies. For osteocalcin and beta-catenin staining, we used 10 ng/ml proteinase K in Tris-EDTA buffer (pH=8.0) for 20 min in a 37°C water bath. For pSMAD5 and proliferation cell nuclear antigen (PCNA) immunohistochemistry staining, we used heat-mediated antigen retrieval in 10 mM citrate buffer (pH=6.0) in a 96°C water bath for 20 minutes. After antigen retrieval, slides were washed in phosphate buffered saline (PBS, pH=7.4) and blocked with 5% donkey serum. Then, primary antibodies were applied and incubated overnight at 4°C. The primary antibodies and dilutions used in this study were as follows: goat anti-mouse osteocalcin (1:50, sc23-790, Santa Cruz Biotechnology, Inc.), rabbit anti-mouse pSMAD5 (1:200, ab92698, Abcam), and anti-mouse β-catenin (1:500, ab16051, Abcam) and rabbit anti-PCNA (1:4000, ab18-197, Abcam). The following day, after PBS washing, slides were incubated with 0.5% H_2O_2 for 30 min at room temperature (RT), then washed in PBS, and the corresponding secondary anti-goat (BA-9500) or anti-rabbit (1:200, BA-1000, Vector Laboratories, Burlingame, CA, USA) biotin-labeled antibodies was applied and incubated for 2 h at RT. After washing with PBS, each slide was incubated in ABC reagent (PK 7200, Elite ABC kits, Vector Laboratories) for 1 h at RT. Then, a DAB staining kit (SK-4100, Vector Laboratories) was used to reveal the positive cells (brown color). Hematoxylin (H-3404, Vector Laboratories) was used to counterstain the nuclei. Finally, each slide was hydrated through an ethanol gradient, cleared with xylene, and mounted in Cytoseal mount medium.

Tartrate-resistant acid phosphatase (TRAP) staining for OCs was also performed on the decalcified paraffin sections using a 387A kit (Sigma, Milwaukee, USA) [18]. Briefly, slides were incubated with solution mixed with fast Garnet solution, acetate solution, Naphthol AS-BI phosphatase solution and Tartrate acid solution for 1 hour at 37°C, then the slides were counterstained for 2 min with hematoxylin and mounted with Permafluor aqueous mount medium (TA-030-FM, Thermo-Fisher Scientific). The microscopic images were obtained using NIKON NIS software (Nikon, Melville, NY, USA).

pSMAD5 staining was used to detect BMP signaling. β-catenin staining was used to reveal Wnt/β-catenin signaling. Osteocalcin and TRAP staining were performed for detection of OBs and OCs, respectively.

For the 6-week calluses, H&E, Herocivi's, TRAP, and osteocalcin staining were performed to investigate the fracture healing. H&E, Alcian blue, Herocivi's, osteocalcin, pSMAD5, and β-catenin staining were performed on the 10-day samples to explore the mechanisms of gender differences during fracture healing. To quantify the positive-staining cell numbers, 6-8 200× images were taken to cover the whole view of the callus for 6-week calluses. For the 10-day calluses, TRAP-positive and osteocalcin-positive cells were counted on the regenerated bone surface using Image J. The number of positive cells was normalized to 200× bone area for each sample for statistical analysis between groups.

RNA isolation and RT-qPCR

Total RNA was extracted from the 10-day callus homogenate (6 male and 6 female per group) using Trizol Reagent (Invitrogen, Life Technologies, Carlsbad, CA). For real-time quantitative RT-PCR (RT-qPCR) analysis, RNA was reverse-transcribed to cDNA using an iScript Reverse Transcription Supermix for RT-qPCR kit (170-8841, Bio-Rad). The qPCR was carried out to detect expression of several osteogenic-related gene markers using the SsoAdvanced™ Universal SYBR® Green Supermix (BIO-RAD) and using the CFX Connect™ Real-Time PCR Detection System (Bio-Rad, Inc., Hercules, CA). Glyceraldehyde-3-phosphate dehydrogenase (GAPDH) was used as an internal control for each sample. Primers were designed using Primer 3 Input according to literature [21, 22]. Primer sequences are listed in **Table 1**. Target gene mRNA expression was normalized to GAPDH expression and expressed as the fold change versus male group of control or *mdx* group for each experimental group.

Table 1. Primer information

Gene Names	Accession numbers	Forward primers (5'-3')	Reverse Primers (5'-3')	Product size (bp)
IGF1	NM_010512.5	tggatgctcttcagttcgtg	gcaacactcatccacaatgc	173
IGF2	NM_010514.3	gtcgatgttggtgcttctca	aagcagcactcttccacgat	185
OSX	AF184902	actcatccctatggctcgtg	ggtagggagctgggttaagg	238
ALP	BC065175	gctgatcattcccacgtttt	ctgggcctggtagttgttgt	204
BMP2	BC100344.1	tgcaccaagatgaacacagc	gtgccacgatccagtcattc	201
BMP4	BC052846	ggttcctggacacctcatca	ctgattctgacatgctggcc	195
BMP6	BC138593	tctacaacgccctgtccaat	tgtcgttgatgtggggagaa	283
BMP7	BC010771	cccagaacaagcaacccttc	tggtcactgctgctgttttc	169
BMP9	AF188286	gacagtgagacttgggacca	ctggtctccttggtcccatt	275

Statistical analysis

All values are expressed as the mean ± standard deviation (SD). The Student's t-test was used to determine differences between two groups. $P<0.05$ was considered statistically significant. For the data that had high standard deviations, the Wilcoxon Rank sum non-parametric test was utilized by ranking the values of all groups and referring the Wilcoxon rank sum table according to each group's sample number. If the sum is larger than the upper tail or smaller than the lower tail probability value (0.05 or less), they are considered statistically different.

Results

Male mice formed larger bone callus with lower density when compared to female mice

3D microCT images showed that fracture sites were almost healed at 6 weeks after surgery in WT and *mdx* mice independent of the gender. The fractures in female mice healed faster and remodeled better compared to males for both WT and *mdx* mice (**Figure 1A**). The microCT 3D images showed that, while the calluses in males were larger in size, the newly regenerated bone was thin and sparse when compared to that of female mice. Conversely, the bone calluses in female mice were thicker and denser compared to the calluses in male mice for both WT and *mdx* mice (**Figure 1B**). MicroCT quantification indicated the male *mdx* mice had higher total volume (TV) at all time points (**Figure 1C**) and higher bone volume (BV) at 6 weeks (**Figure 1D**), which means larger callus size than female *mdx* mice. However, the female *mdx* mice had a higher BV/TV ratio and density at all time points, indicating better quality of callus when compared to that of male *mdx* mice (**Figure 1E**, **1F**). Higher Tb.N and lower Tb.Sp was observed in females, which indicates that their calluses contain more trabecular bone compared to male mice (**Figure 1G**, **1H**). Likewise, in WT mice, males had higher TV and BV at 4 and 6 weeks (**Figure 1C**, **1D**), while females had higher BV density at 2 and 4 weeks (**Figure 1F**). However, the calluses in female mice demonstrated superior remodeling when compared to those in male mice for both WT and *mdx* mice.

Callus of female mice remodeled better due to a high number of OCs when compared to male mice

At 6 weeks after fracture, H&E staining showed that calluses of the male mice were larger, but mostly consisted of trabecular bone, when compared to female for both WT and *mdx* mice. The calluses of female mice (WT and *mdx*) were relatively smaller in size, but contained more cortical bone-like architecture than those of male mice (**Figure 2A**). Consequently, the cortical bone in calluses in male groups was thinner than in the female groups for both WT and *mdx* mice as revealed by Herovici's staining (**Figure 2B**). TRAP staining indicated more TRAP-positive OCs in the calluses of female WT and *mdx* mice than their male counterparts (**Figure 2C**, **2E**). No gender differences were found in the number of osteocalcin-positive OBs in WT and *mdx* mice.

Male mice formed larger calluses but female mice showed faster bone formation

At 10 days after fracture, similar to findings at 6 weeks, H&E staining demonstrated that, in both WT and *mdx* mice, male mice always had

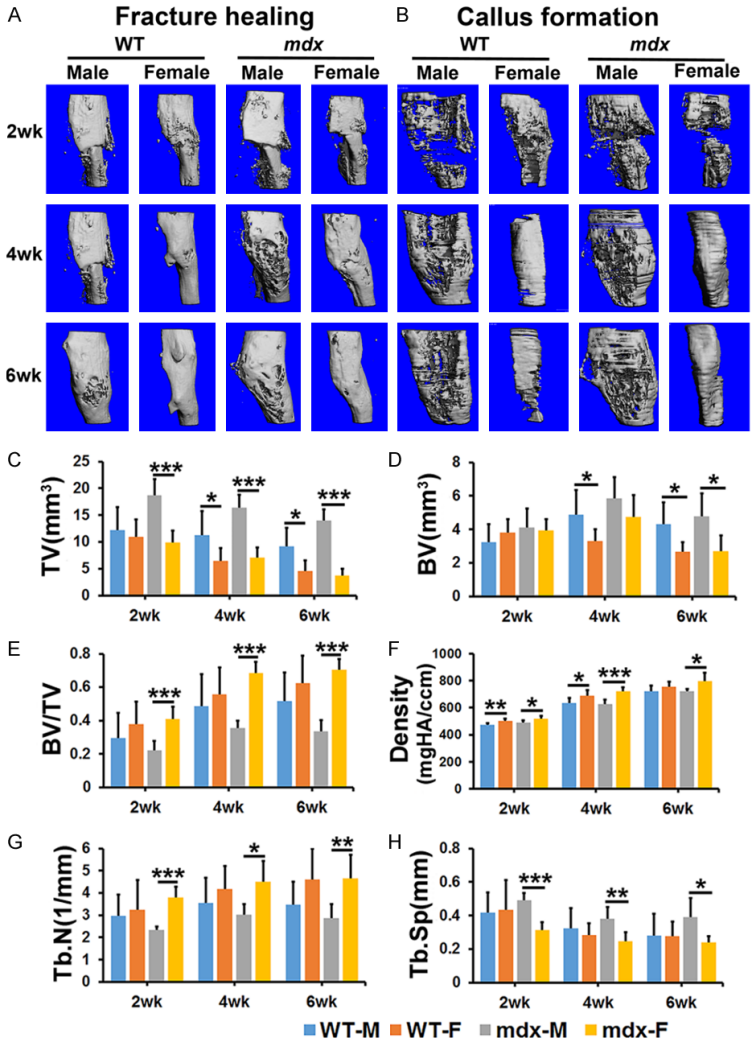

Figure 1. MicroCT 3D images and quantification of tibial fracture healing of male and female wild-type (WT) and *mdx* mice at different time points after injury. A. MicroCT 3D images showed the tibial fractures in female mice healed faster and remodeled better compared to males for both WT and *mdx* mice at all time points. B. MicroCT 3D images of calluses showed that the calluses in males were larger in size with lower density, while the calluses in female mice were smaller but with higher density for both WT and *mdx* mice at all time points. C. MicroCT quantification indicated the male *mdx* mice had higher total volume (TV) at all time points while male normal and *mdx* mice showed significantly bigger calluses at 4 and 6 weeks after surgery. D. The male *mdx* mice had higher bone volume (BV) at 6 weeks. E. The male *mdx* mice had lower BV/TV ratio at all time points. F. The male *mdx* mice had lower density at all time points. G. The male *mdx* mice had lower trabecular number (Tb.N) at all time points. H. The male *mdx* mice showed higher trabecular separation (Tb.Sp) at all time points. **P*<0.05, ***P*<0.01, ****P*<0.001.

larger calluses, which consisted of mainly trabecular bone surrounding the broken native bone. The soft callus showed light blue staining while native bone showed red staining. The broken ends of the bone were not connected yet for both male and female mice (**Figure 3A**). Herovici's staining showed red bone matrices formed surrounding the broken end of the tibia in both groups at the 10-day time point, but the female mice showed more trabecular bone (red color) than male mice in both WT and *mdx* mice (**Figure 3B**). Alcian blue staining showed endochondral bone formation in both groups independent of gender. The calluses from WT male contained a higher percentage of mesenchyme, while the calluses from the female counterparts contained a lower percentage of bone. In *mdx* mice, the percentage of cartilage was smaller in the calluses of female mice than those of male mice, while no differences were found for the percentage of bone and mesenchyme in female *mdx* mice compared to male *mdx* mice (**Figure 3C**, **3D**).

The Wnt/β-catenin signaling pathway was upregulated which contributed to the higher number of OBs

We further investigated what signaling pathways contributed to the gender difference. We found, more OBs in the calluses of male mice compared to those of females in WT and *mdx* mice in 10-day calluses (**Figure 4A**, **4B**). More β-catenin-positive cells (activated non-phosphorylated form) were also detected in the male WT and *mdx* mice, indicating a higher level of activation of the Wnt/β-catenin signaling pathway during callus formation in male mice (**Figure 4C**, **4D**). We investigated the BMP/pSMAD signaling pathway by performing pSMAD 5 staining. No gender differences were found for the numbers of pSMAD5-positive cells in both WT and *mdx* mice (**Figure 4E**, **4F**).

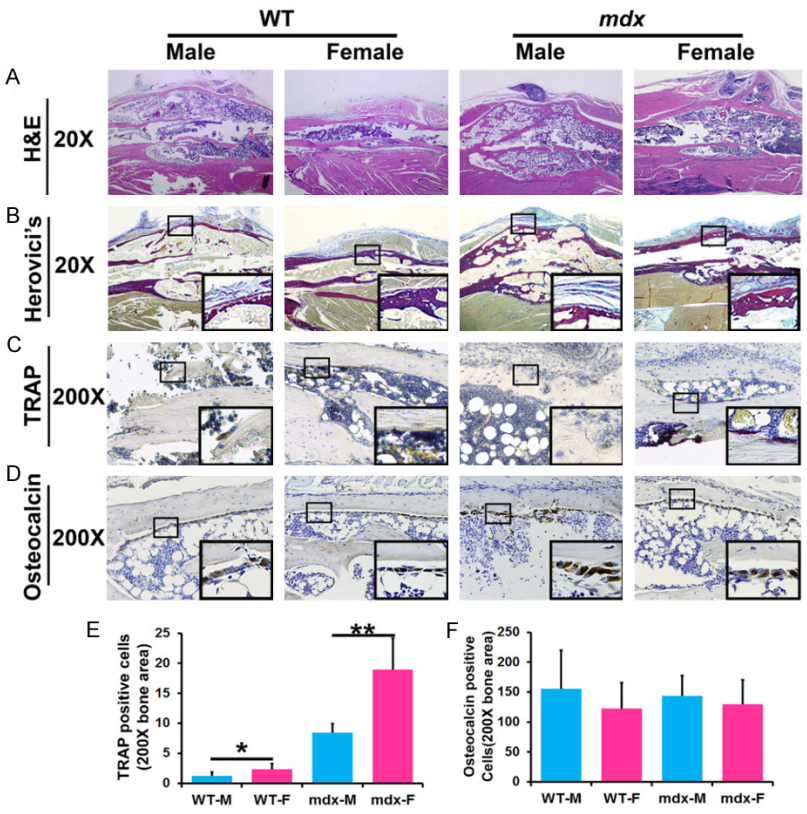

Figure 2. Histology of tibial fracture healing of male and female wild-type (WT) and *mdx* mice at 6 weeks after surgery. A. Hematoxylin and eosin (H&E) staining showed that calluses of the males were composed mostly of trabecular bone whereas, the female groups had already formed cortical bone-like architecture. B. Herovici's staining showed the formation of bone matrix collagen I (red color). The collagen I-positive bone calluses were smaller in female mice than male mice in both the WT and *mdx* groups. The cortical bone in the male groups was thinner than in the female groups, both in the WT and *mdx* mice. C, E. TRAP staining for osteoclasts (OC) and quantification at 6 weeks after surgery. More OCs were observed in calluses of female mice than in male mice in both the WT and *mdx* mice. D, F. Osteocalcin staining for osteoblasts and quantification at 6 weeks after fracture. No gender differences were found in osteoblasts (OBs) in WT and *mdx* mice. **P*<0.05, ***P*<0.01.

No difference with cell proliferation between male and female mice for either WT or mdx mice

We further performed PCNA immunohistochemistry staining to investigate cell proliferation for 10 days tibia fracture tissues. We quantified the PCNA positive cells for bone area and cartilage area in the calluses. We found a trend of increase of PCNA positive cells in the bone area of WT female mice than the male mice (P= 0.062), but not reach statisitical difference (**Figure 5A**, **5C**). No statisitical difference was detected for the number of PCNA positive cells between mdx male and female mice. We also found no significant differences of the number of PCNA positive cells between male and female mice for either WT or *mdx* mice in the cartilage area (**Figure 5B**, **5C**).

Male mice showed relative Higher IGF-1 expression, while females mice had higher BMP-9 level during fracture healing

Next, we performed RT-qPCR for osteogenic related genes for 10 days fracture calluses. RT-qPCR results demonstrated higher IGF-1 expression in calluses of male *mdx* mice, while females demonstrated higher BMP-9 expression in WT mice. No gender differences were found for IGF-2, OSX, ALP, and BMP 2, 4, 6, and 7 expression levels in either WT or *mdx* mice (**Figure 6**).

Discussion

In this study, we found that both male and female WT and *mdx* mice achieved almost complete healing at the fracture site by 6 weeks after injury. During the fracture healing process, the bone callus formation in female mice at a faster rate with a more complete remodelling when compared to their male counterparts in both WT and *mdx* groups. This was revealed by higher BV/TV ratio, density, and Tb.N as measured by microCT analyses. Male mice exhibited larger callus size with higher TV and BV values than their female counterparts in both WT and *mdx* mice at 4 and 6 weeks after fracture. At 6 weeks after fracture, histology revealed that, although male mice (both WT and *mdx*) had larger calluses, the female calluses had thicker cortical bone, which showed superior remodeling and increased bone matrix collagen I expression. The improved remodeling of bone calluses in female mice may be attributed to more OCs generated during fracture healing.

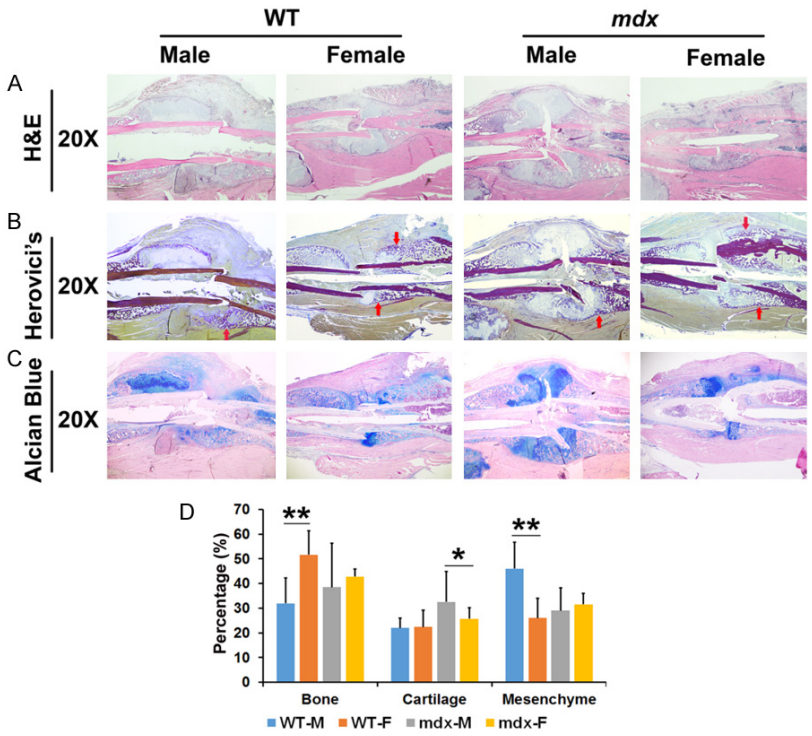

Figure 3. Histology of tibial fracture healing at 10 days after surgery. A. Hematoxylin and eosin (H&E) staining showed the formation of calluses in each group. Female mice had smaller calluses than male mice, and none of the fractures were healed at this time point. B. Herovici's staining showed bony calluses (red color) in each group surrounding the broken native cortical bone, and female calluses appeared to have more trabecular bone formed, which indicated a faster healing process than in male mice (red arrows). C, D. Alcian blue staining and quantification. Female mice appeared to exhibit smaller cartilage areas (blue matrix) than male mice in both wild-type (WT) and *mdx* groups. The calluses of WT female mice showed higher bone percentages and lower mesenchyme percentages than those of male mice, which indicated a faster bone healing process. The calluses of female *mdx* mice exhibited lower cartilage percentages than those of male *mdx* mice. No differences were found for bone and mesenchyme percentages between male and female *mdx* mice. **P*<0.05, ***P*<0.01.

No gender differences were found in OB numbers in the bone fracture at 6 weeks post-injury for either WT or *mdx* mice. The gender differences between males and females were not attributed to cells proliferation during fracture healing.

Fracture repair requires the mobilization and involvement of multiple cell types and signaling pathways at the injury site [23]. Long-bone fracture repair occurs through a process of endochondral ossification. Initiation of the fracture healing process involves recruitment of mesenchymal progenitor cells, especially from the periosteum, to the injury site and differentiation. Cells undergo chondrogenesis, connecting the gap between the injured bone with a soft callus composed of cartilaginous matrix. After hypertrophy of the chondrocytes and calcification of the cartilage callus, osteoprogenitor cells are recruited to the callus site, resulting in osteoblastic differentiation and mineralization onto the calcified cartilage. The process of calcified cartilage remodeling and replacement of the soft callus with bony callus, results in completely new bone tissue that mimics the structure, features, and components prior to injury [24, 25].

To determine potential mechanisms of gender differences of fracture healing, we sacrificed mice at an early stage (10 days) of callus formation post-injury, and found that female calluses contained a higher percentage of bone tissue, which indicates a faster transformation from cartilage to bone. By contrast, a lower percentage of mesenchyme was detected in the callus of female mice. However, our results contradict a previous study that demonstrated female rats had inferior fracture healing compared to male rats in a femur gap model, which was associated with decreased bone marrow colony-forming units [26]. The discrepancy between this previous study and ours might be related to the fact that we used a different species or animals of different ages [26].

The initiation of bone fracture repair requires differentiation of MSCs into an osteochondral lineage, a process which is tightly regulated by canonical Wnt/β-catenin signaling [27, 28]. In our study, we found more β-catenin-positive cells in the bone fracture area of male mice at 10 days post-injury in both normal mice and *mdx* mice compared to females at that time point, which might explain why males formed larger calluses. This finding also correlates with

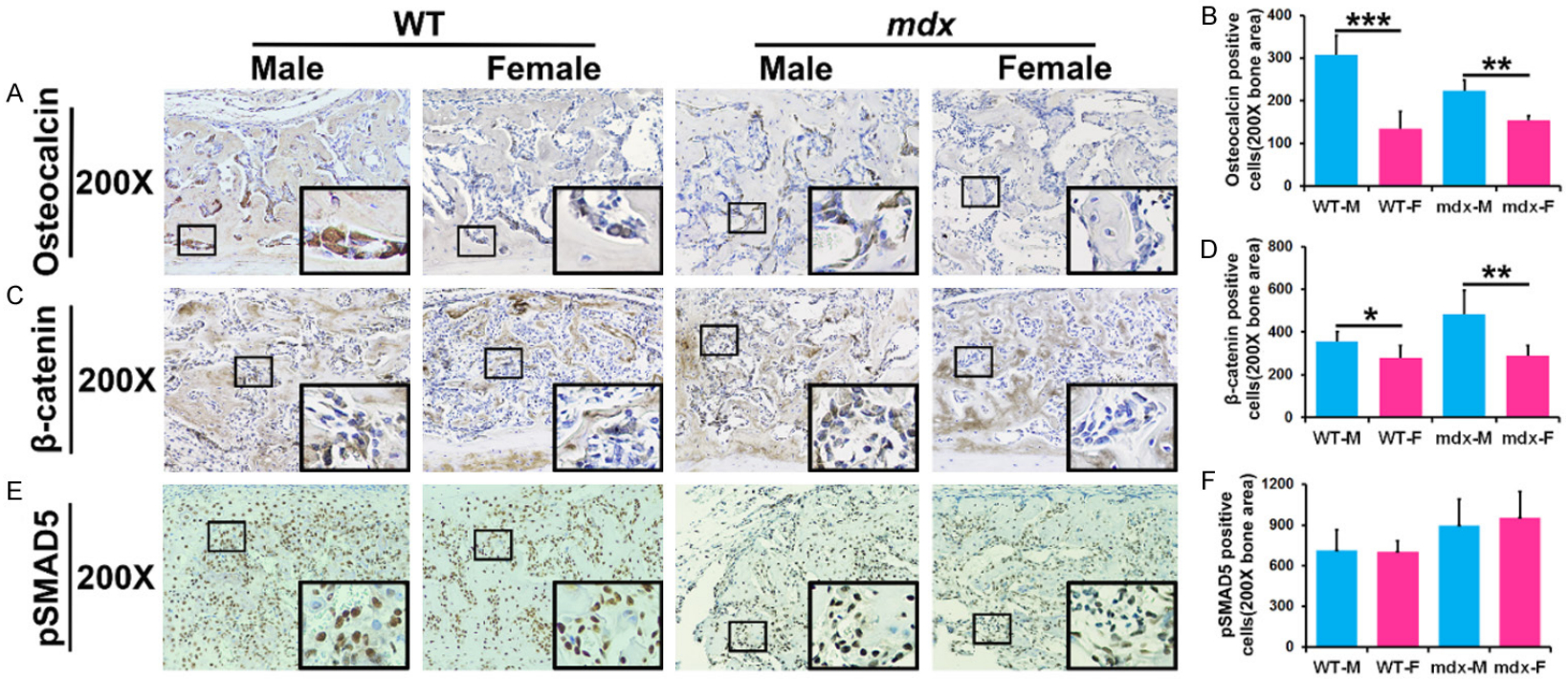

Figure 4. Immunohistochemistry of tibial fracture tissues at 10 days after surgery. A, B. Osteocalcin staining and quantification at 10 days after surgery. Fewer osteocalcin-positive osteoblasts (OBs) were detected in the female wild-type (WT) and dystrophic (*mdx*) mice than in their male counterparts. C, D. β-catenin staining and quantification. Fewer β-catenin-positive cells were detected in the female WT and *mdx* mice than in the male WT and *mdx* mice. E, F. pSMAD5 staining and quantification. No significant gender differences were observed in the number of pSMAD5-positive cells in either WT or *mdx* mice. **P*<0.05, ***P*<0.01, ****P*<0.001.

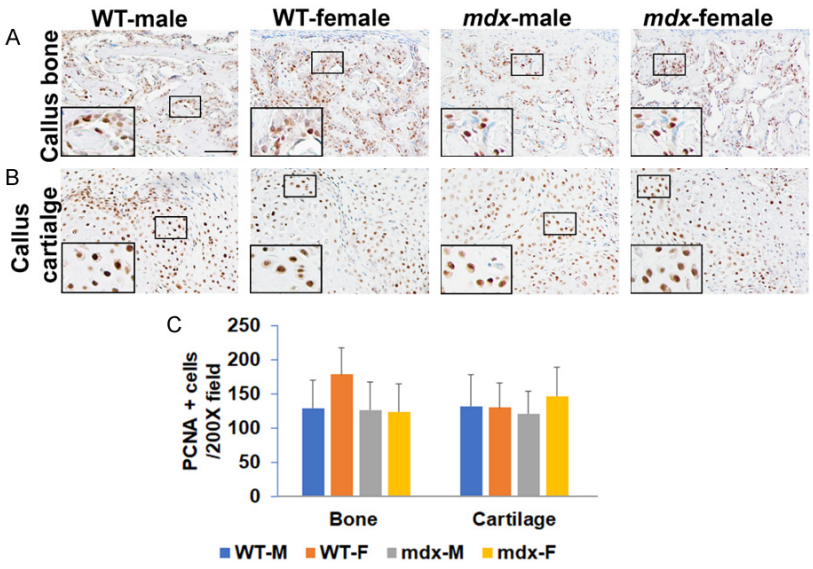

Figure 5. Immunohistochemistry staining of cell proliferation marker PCNA at 10 days post-fracture. A. PCNA staining of the callus bone area for 4 different groups. Brown color showed PCNA positive cells. Insets are the enlarged box area in each image. B. PCNA staining of callus cartilage area for 4 different groups. Brown color showed PNCA positive cells. Insets are the enlarged box area in each image. C. Quantification of PCNA positive cells in the bone and cartilage area of tibia fracuture calluses. No statistical difference was found between male and female mice for WT and *mdx* mice groups for either bone or cartilage area. Scale bar=100 μm for all images.

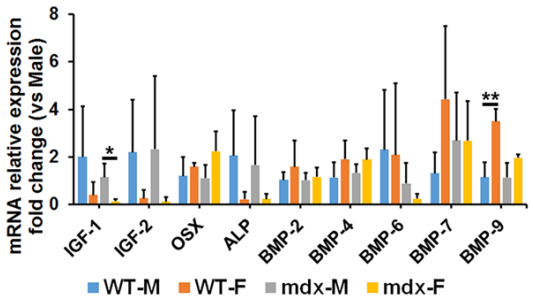

Figure 6. RT-qPCR to measure expression of osteogenesis-related genes in the calluses at 10 days after fracture surgery in male and female wild-type (WT) and *mdx* mice. Significantly higher IGF-1 expression was detected in male compared to female *mdx* mice. IGF-2 also showed trends of elevation in male mice compared to female mice in both WT and mdx groups. In addition, female WT mice showed significant higher BMP-9 expression compared to male WT mice. No statistically significant gender differences were found for other genes. **P*<0.05, ***P*<0.01.

more OBs in the male calluses, at this early time point post-injury. Previous studies have demonstrated the significance of canonical Wnt/β-catenin signaling in osteogenesis and chondrogenesis by emphasizing that precise levels of β-catenin stabilization are required during different stages of MSC differentiation toward the osteochondral lineage [29-31]. Furthermore, inhibition of the Wnt/β-catenin signaling pathway delays fracture union, which is associated with decreased cartilage formation, cartilage hypotrophy and, bone formation [32]. These results taken together suggest that gender differences in the canonical Wnt/β-catenin signaling pathway could explain the corresponding differences in callus formation.

Bone morphogenetic proteins (BMPs) were named for their ability to induce bone and cartilage formation and they play critical roles in cartilage and bone formation during skeletal development and repair [33]. However, no gender differences in numbers of pSMAD5-positive cells were found in both WT and *mdx* mice, which indicates pSMAD5-BMP signaling may not play a key role in the gender differences in normal and *mdx* mice bone healing.

It is known that the BMP/pSMAD5 signaling pathway is critical for all bone fracture healing [34]. BMP-9 has been shown to be one of the most potent BMPs in inducing osteogenic differentiation and bone formation of MSCs *in vitro* and *in vivo* [35, 36]. In this study, we detected higher BMP-9 expression in WT female 10-day calluses when compared to male WT mice. Female *mdx* mice also exhibited relatively higher BMP9 expression levels in fracture calluses at 10 days post-surgery. It has recently been shown in a study characterizing circulating BMPs in patients who have demonstrated normal or delayed fracture healing, that circulating BMP concentrations were not significantly different between the groups [37]. However, they inferred that increased circulating BMP-9 levels seem to be associated with faster fracture healing [37]. Thus, the correlation between BMP-9 levels and fracture healing needs to be further investigated to elu-

cidate a role in the differential bone healing process between genders.

Interestingly, we found both WT and *mdx* female mice had relatively higher expression of osterix (OSX), a key transcription factor of osteogenic differentiation (P=0.066), which has been demonstrated playing an important role in mediating endochondral ossification during fracture repair [38]. The relatively higher OSX expression in female mice may indicate faster osteogenic differentiation, which correlated with better bone quality (BV/TV) in female mice.

Furthermore, we found IGF-1 expression was upregulated in male *mdx* mice when compared to their female counterparts which may play a role in the larger callus observed in these male mice. IGF-1 expression was also increased in WT male mice when compared to their female counterpart although the difference was not significant. IGF-1 is the most abundant growth factor stored in bone matrix, and is involved in both bone development and remodeling [39]. Impairment of the growth hormone (GH)/IGF-1 axis affects the quality of fracture healing, indicating it plays an important role in fracture healing [40]. Lower concentration of serum IGF-1 was detected in non-union groups of trauma patients compared with union groups [40]. IGF-1 is involved in cell proliferation and differentiation of mesenchymal cells, periosteal cells, OBs, and chondrocytes during fracture healing [41]. Evidence accumulates on the communication between these cells, which are biologically tightly connected to fracture healing. It has been proven that IGF-1 can regulate proliferation, differentiation, and survival of OBs, as well as bone matrix synthesis, which promote fracture repair [41-43].

One of the limitations of the current study is that the conclusion was based on relatively young mice (2-month-old). Additional studies would be needed to determine whether this gender difference in fracture repair is also observed in aged/old mice, and increasing our understanding of the effect of age on bone healing [44]. Another limitation is that the RT-qPCR showed a very high standard deviation for the 10-day post-fracture calluses. The incomplete removal of the surrounding tissues, such as skeletal muscle, may have contributed to this high variability. Despite these limitations, our findings confirm gender differences during fracture healing in WT and *mdx* mice.

Conclusions

Male mice formed larger bone calluses during tibial fracture healing in WT and *mdx* mice, which may be attributed to higher IGF-1 expression, higher activation of Wnt/β-catenin signaling pathway and greater OB numbers during callus formation. Female mice achieved better morphology in the healed fractured bone with higher bone quality due to the greater number of OCs increased bone remodeling and higher BMP-9 expression levels. These results further validate that gender is one of many variables that needs to be considered in animal and human studies for bone research.

Acknowledgements

This project is supported by an NIH grant awarded to Dr. Johnny Huard (5R01AR065445). We thank Dr. Mary A. Hall and Anna-Laura Nelson, M.S for proofreading and scientific editing. We also thank Mrs. Ruth McCarrick for English editing during revision.

Disclosure of conflict of interest

None.

Address correspondence to: Dr. Johnny Huard, Center for Regenerative Sports Medicine, The Steadman Philippon Research Institute, 181 W Meadow Dr, Vail, CO 81657, USA. E-mail: jhuard@sprivail.org; Dr. Xueqin Gao, Center for Regenerative Sports Medicine Fort Collins Laboratory, The Steadman Philippon Research Institute, 702 W Drake Road, Building G101, Fort Collins, CO 80526, USA. E-mail: xgao@sprivail.org

References

[1] Govoni A, Magri F, Brajkovic S, Zanetta C, Faravelli I, Corti S, Bresolin N and Comi GP. Ongoing therapeutic trials and outcome measures for Duchenne muscular dystrophy. Cell Mol Life Sci 2013; 70: 4585-4602.

[2] McDonald DG, Kinali M, Gallagher AC, Mercuri E, Muntoni F, Roper H, Jardine P, Jones DH and Pike MG. Fracture prevalence in Duchenne muscular dystrophy. Dev Med Child Neurol 2002; 44: 695-698.

[3] Perera N, Sampaio H, Woodhead H and Farrar M. Fracture in duchenne muscular dystrophy: natural history and vitamin D deficiency. J Child Neurol 2016; 31: 1181-1187.

[4] Larson CM and Henderson RC. Bone mineral density and fractures in boys with Duchenne

muscular dystrophy. J Pediatr Orthop 2000; 20: 71-74.
[5] Duan D. Challenges and opportunities in dystrophin-deficient cardiomyopathy gene therapy. Hum Mol Genet 2006; 15: R253-261.
[6] Abou-Khalil R, Yang F, Mortreux M, Lieu S, Yu YY, Wurmser M, Pereira C, Relaix F, Miclau T, Marcucio RS and Colnot C. Delayed bone regeneration is linked to chronic inflammation in murine muscular dystrophy. J Bone Miner Res 2014; 29: 304-315.
[7] Bulfield G, Siller WG, Wight PA and Moore KJ. X chromosome-linked muscular dystrophy (mdx) in the mouse. Proc Natl Acad Sci U S A 1984; 81: 1189-1192.
[8] Nakagaki WR, Bertran CA, Matsumura CY, Santo-Neto H and Camilli JA. Mechanical, biochemical and morphometric alterations in the femur of mdx mice. Bone 2011; 48: 372-379.
[9] Corsi KA, Pollett JB, Phillippi JA, Usas A, Li G and Huard J. Osteogenic potential of postnatal skeletal muscle-derived stem cells is influenced by donor sex. J Bone Miner Res 2007; 22: 1592-602.
[10] Matsumoto T, Kubo S, Meszaros LB, Corsi KA, Cooper GM, Li G, Usas A, Osawa A, Fu FH and Huard J. The influence of sex on the chondrogenic potential of muscle-derived stem cells: implications for cartilage regeneration and repair. Arthritis Rheum 2008; 58: 3809-3819.
[11] Meszaros LB, Usas A, Cooper GM and Huard J. Effect of host sex and sex hormones on muscle-derived stem cell-mediated bone formation and defect healing. Tissue Eng Part A 2012; 18: 1751-1759.
[12] Lau KW, Rundle CH, Zhou XD, Baylink DJ and Sheng MH. Conditional deletion of IGF-I in osteocytes unexpectedly accelerates bony union of the fracture gap in mice. Bone 2016; 92: 18-28.
[13] Bouxsein ML, Boyd SK, Christiansen BA, Guldberg RE, Jepsen KJ and Muller R. Guidelines for assessment of bone microstructure in rodents using micro-computed tomography. J Bone Miner Res 2010; 25: 1468-1486.
[14] Dempster DW, Compston JE, Drezner MK, Glorieux FH, Kanis JA, Malluche H, Meunier PJ, Ott SM, Recker RR and Parfitt AM. Standardized nomenclature, symbols, and units for bone histomorphometry: a 2012 update of the report of the ASBMR Histomorphometry Nomenclature Committee. J Bone Miner Res 2013; 28: 2-17.
[15] Levame M and Meyer F. Herovici's picropolychromium. Application to the identification of type I and III collagens. Pathol Biol (Paris) 1987; 35: 1183-1188.
[16] Turner NJ, Pezzone MA, Brown BN and Badylak SF. Quantitative multispectral imaging of Herovici's polychrome for the assessment of collagen content and tissue remodelling. J Tissue Eng Regen Med 2013; 7: 139-148.
[17] Gao X, Usas A, Lu A, Kozemchak A, Tang Y, Poddar M, Sun X, Cummins JH and Huard J. Cyclooxygenase-2 deficiency impairs muscle-derived stem cell-mediated bone regeneration via cellular autonomous and non-autonomous mechanisms. Hum Mol Genet 2016; 25: 3216-3231.
[18] Gao X, Usas A, Tang Y, Lu A, Tan J, Schneppendahl J, Kozemchak AM, Wang B, Cummins JH, Tuan RS and Huard J. A comparison of bone regeneration with human mesenchymal stem cells and muscle-derived stem cells and the critical role of BMP. Biomaterials 2014; 35: 6859-6870.
[19] Zhang X, Schwarz EM, Young DA, Puzas JE, Rosier RN and O'Keefe RJ. Cyclooxygenase-2 regulates mesenchymal cell differentiation into the osteoblast lineage and is critically involved in bone repair. J Clin Invest 2002; 109: 1405-1415.
[20] Naik AA, Xie C, Zuscik MJ, Kingsley P, Schwarz EM, Awad H, Guldberg R, Drissi H, Puzas JE, Boyce B, Zhang X and O'Keefe RJ. Reduced COX-2 expression in aged mice is associated with impaired fracture healing. J Bone Miner Res 2009; 24: 251-264.
[21] Untergasser A, Cutcutache I, Koressaar T, Ye J, Faircloth BC, Remm M and Rozen SG. Primer3--new capabilities and interfaces. Nucleic Acids Res 2012; 40: e115.
[22] Koressaar T and Remm M. Enhancements and modifications of primer design program primer3. Bioinformatics 2007; 23: 1289-1291.
[23] Kumagai K, Vasanji A, Drazba JA, Butler RS and Muschler GF. Circulating cells with osteogenic potential are physiologically mobilized into the fracture healing site in the parabiotic mice model. J Orthop Res 2008; 26: 165-175.
[24] Marsell R and Einhorn TA. The biology of fracture healing. Injury 2011; 42: 551-555.
[25] Marzona L and Pavolini B. Play and players in bone fracture healing match. Clin Cases Miner Bone Metab 2009; 6: 159-162.
[26] Strube P, Mehta M, Baerenwaldt A, Trippens J, Wilson CJ, Ode A, Perka C, Duda GN and Kasper G. Sex-specific compromised bone healing in female rats might be associated with a decrease in mesenchymal stem cell quantity. Bone 2009; 45: 1065-1072.
[27] Hill TP, Spater D, Taketo MM, Birchmeier W and Hartmann C. Canonical Wnt/beta-catenin signaling prevents osteoblasts from differentiating into chondrocytes. Dev Cell 2005; 8: 727-738.
[28] Baksh D, Boland GM and Tuan RS. Cross-talk between Wnt signaling pathways in human mesenchymal stem cells leads to functional

antagonism during osteogenic differentiation. J Cell Biochem 2007; 101: 1109-1124.
[29] Day TF, Guo X, Garrett-Beal L and Yang Y. Wnt/beta-catenin signaling in mesenchymal progenitors controls osteoblast and chondrocyte differentiation during vertebrate skeletogenesis. Dev Cell 2005; 8: 739-750.
[30] Silkstone D, Hong H and Alman BA. Beta-catenin in the race to fracture repair: in it to Wnt. Nat Clin Pract Rheumatol 2008; 4: 413-419.
[31] Lauing KL, Roper PM, Nauer RK and Callaci JJ. Acute alcohol exposure impairs fracture healing and deregulates beta-catenin signaling in the fracture callus. Alcohol Clin Exp Res 2012; 36: 2095-2103.
[32] Huang Y, Zhang X, Du K, Yang F, Shi Y, Huang J, Tang T, Chen D and Dai K. Inhibition of beta-catenin signaling in chondrocytes induces delayed fracture healing in mice. J Orthop Res 2012; 30: 304-310.
[33] Deng ZH, Li YS, Gao X, Lei GH and Huard J. Bone morphogenetic proteins for articular cartilage regeneration. Osteoarthritis Cartilage 2018; 26: 1153-1161.
[34] Prall WC, Haasters F, Heggebo J, Polzer H, Schwarz C, Gassner C, Grote S, Anz D, Jäger M, Mutschler W and Schieker M. Mesenchymal stem cells from osteoporotic patients feature impaired signal transduction but sustained osteoinduction in response to BMP-2 stimulation. Biochem Biophys Res Commun 2013; 440: 617-622.
[35] Luu HH, Song WX, Luo X, Manning D, Luo J, Deng ZL, Sharff KA, Montag AG, Haydon RC and He TC. Distinct roles of bone morphogenetic proteins in osteogenic differentiation of mesenchymal stem cells. J Orthop Res 2007; 25: 665-677.
[36] Chen L, Jiang W, Huang J, He BC, Zuo GW, Zhang W, Luo Q, Shi Q, Zhang BQ, Wagner ER, Luo J, Tang M, Wietholt C, Luo X, Bi Y, Su Y, Liu B, Kim SH, He CJ, Hu Y, Shen J, Rastegar F, Huang E, Gao Y, Gao JL, Zhou JZ, Reid RR, Luu HH, Haydon RC, He TC and Deng Z. Insulin-like growth factor 2 (IGF-2) potentiates BMP-9-induced osteogenic differentiation and bone formation. J Bone Miner Res 2010; 25: 2447-2459.
[37] van Baardewijk LJ, van der Ende J, Lissenberg-Thunnissen S, Romijn LM, Hawinkels LJ, Sier CF and Schipper IB. Circulating bone morphogenetic protein levels and delayed fracture healing. Int Orthop 2013; 37: 523-527.
[38] Kaback LA, Soung do Y, Naik A, Smith N, Schwarz EM, O'Keefe RJ and Drissi H. Osterix/Sp7 regulates mesenchymal stem cell mediated endochondral ossification. J Cell Physiol 2008; 214: 173-182.
[39] Xian L, Wu X, Pang L, Lou M, Rosen CJ, Qiu T, Crane J, Frassica F, Zhang L, Rodriguez JP, Jia X, Yakar S, Xuan S, Efstratiadis A, Wan M and Cao X. Matrix IGF-1 maintains bone mass by activation of mTOR in mesenchymal stem cells. Nat Med 2012; 18: 1095-1101.
[40] Weiss S, Henle P, Bidlingmaier M, Moghaddam A, Kasten P and Zimmermann G. Systemic response of the GH/IGF-I axis in timely versus delayed fracture healing. Growth Horm IGF Res 2008; 18: 205-212.
[41] Wang T, Wang Y, Menendez A, Fong C, Babey M, Tahimic CG, Cheng Z, Li A, Chang W and Bikle DD. Osteoblast-specific loss of IGF1R signaling results in impaired endochondral bone formation during fracture healing. J Bone Miner Res 2015; 30: 1572-1584.
[42] Bikle D, Majumdar S, Laib A, Powell-Braxton L, Rosen C, Beamer W, Nauman E, Leary C and Halloran B. The skeletal structure of insulin-like growth factor I-deficient mice. J Bone Miner Res 2001; 16: 2320-2329.
[43] Nakae J, Kido Y and Accili D. Distinct and overlapping functions of insulin and IGF-I receptors. Endocr Rev 2001; 22: 818-835.
[44] Hebb JH, Ashley JW, McDaniel L, Lopas LA, Tobias J, Hankenson KD and Ahn J. Bone healing in an aged murine fracture model is characterized by sustained callus inflammation and decreased cell proliferation. J Orthop Res 2018; 36: 149-158.